$KNd(MoO_4)_2$: A New Incommensurate Modulated Structure in the Scheelite Family

Vladimir A. Morozov,[†,‡] Alla V. Arakcheeva,[§,||] Gervais Chapuis,[||] Nicolas Guiblin,[||] Marta D. Rossell,[‡] and Gustaaf Van Tendeloo*[,‡]

Department of Chemistry, Moscow State University, 119899 Moscow, Russia, EMAT, University of Antwerp, Groenenborgerlaan 171, B-2020, Antwerp, Belgium, Baykov Institute of Metallurgy and Material Sciences, Russian Academy of Sciences, Leninsky prospekt 49, 119991 Moscow, Russia, and Institut de Physique de la Matière Complexe, Ecole Polytechnique Fédérale de Lausanne, Cubotron, 1015 Lausanne, Switzerland

Received March 9, 2006. Revised Manuscript Received June 16, 2006

Potassium neodymium molybdenum oxide, $KNd(MoO_4)_2$, has been synthesized by the solid-state method. The structure and microstructure have been studied by X-ray powder diffraction and transmission electron microscopy (TEM). TEM revealed that the $KNd(MoO_4)_2$ structure is incommensurately modulated. The scheelite-like structure of $KNd(MoO_4)_2$ has been refined from X-ray powder diffraction intensities in the $(3 + 1)D$ superspace group $I2/b(\alpha\beta0)00$ with $a = 5.5202(2)$ Å, $b = 5.33376(5)$ Å, $c = 11.8977(3)$ Å, $\gamma = 90.9591(7)°$, and modulation vector $\mathbf{q} = 0.57789(4)\mathbf{a}^* - 0.14748(6)\mathbf{b}^*$ ($R_P = 3.09\%$, $R_{wP} = 4.04\%$). The ordering of the K and Nd cations appears to be the primary parameter of the structure modulations. The compositional wave of the $\{KMoO_4\}$ and $\{NdMoO_4\}$ distribution is observed in the *ab* structure projection. The incommensurability of the compositional wave direction with respect to the *a* and *b* lattice constants is regarded as the origin of the incommensurate structure modulations.

1. Introduction

The study of new advanced materials for optoelectronic applications has attracted broad interest. Recently increasing attention has been focused on the design and functioning of solid-state lasers.[1] The aim to develop solid-state lasers appears to be important since they are very useful for many applications such as medical treatment or optical communication. They are interesting because of their high stability, compactness, high efficiency, long lifetime, and low cost. Compounds with the scheelite-type structure can be used as potential laser materials. For example, the scheelite-type $MLn(BO_4)_2$ (M = alkali metal (Li, Na, K), Ln = lanthanide, B = W, Mo) single crystals can be considered as interesting self-doubling solid-state laser host materials. For this reason the optical properties of the scheelite-type compounds have been studied extensively in recent years.[2]

The scheelite structure $CaWO_4$ is tetragonal with space group symmetry $I4_1/a$.[3] This structural type is adopted by a large family of compounds with the general composition ABO_4. Many different A and B cations with various oxidation states for both cations may be easily accommodated in the scheelite structure. Some examples illustrate the variety of possible cation oxidation states: $KReO_4$ and $AgIO_4$ (A^+ and B^{7+}), $CdMoO_4$ and $CaMoO_4$ (A^{2+} and B^{6+}), $BiVO_4$ and $YNbO_4$ (A^{3+} and B^{5+}), $ZrGeO_4$ (A^{4+} and B^{4+}). The scheelite-type ABO_4 structure is made up of AO_8 polyhedra and BO_4 tetrahedra sharing common vertices. The edge-sharing AO_8 polyhedra form a 3D framework (Figure 1).

Ca^{2+} in $CaBO_4$ (B = W, Mo) can be substituted by a combination of a monovalent alkali metal and a trivalent cation, leading to the formation of $MR(BO_4)_2$ (M = alkali metal, R = Ln, Y, Bi) compounds with a statistical distribution of M^+ and R^{3+}. The $MLn(MoO_4)_2$ (M = Li, Na) double molybdates with the scheelite-type structure are known for all Ln elements.[4−6] Only $LiLa(MoO_4)_2$ undergoes a phase transition from a low-temperature non-scheelite modification to a high-temperature scheelite-type phase.[7] Other $MLn(MoO_4)_2$ (M = Li, Na) compounds do not exhibit such polymorphism.

* To whom correspondence should be addressed. Phone.: +32-32653262. Fax.: +32-32653257. E-mail: staf.vantendeloo@ua.ac.be.
[†] Moscow State University.
[‡] University of Antwerp.
[§] Russian Academy of Sciences.
[||] Ecole Polytechnique Fédérale de Lausanne.

(1) (a) Pask, H. M.; Piper, J. A. *IEEE J. Quantum Electron.* **2000**, *36*, 949. (b) Grabtchikov, A. S.; Kuzmin, A. N.; Lisinetskii, V. A.; Orlovich, V. A.; Ryabtsev, G. I.; Demidovich, A. A. *Appl. Phys. Lett.* **1999**, *75*, 3742. (c) Basiev, T. T.; Sobol, A. A.; Zverev, P. G.; Osiko, V. V.; Powell, R. C. *Appl. Opt.* **1999**, *38*, 594. (d) Cerny, P.; Jelinkova, H.; Basiev, T. T.; Zverev, P. G. *IEEE J. Quantum Electron.* **2002**, *38*, 1471.
(2) (a) Neeraj, S.; Kijima, N.; Cheetham, A. K. *Chem. Phys. Lett.* **2004**, *387*, 2. (b) Shimamura, K.; Sato, H.; Bensalah, A.; Machida, H.; Sarukura, N.; Fukuda, T. *Opt. Mater.* **2002**, *19*, 109. (c) Cheng, Z.; Lu, Q.; Zhang, S.; Liu, J.; Yi, X.; Song, F.; Kong, Y.; Han, J.; Chen, H. *J. Cryst. Growth* **2001**, *222*, 797. (d) Shi, F.; Meng, J.; Ren, Y.; Su, Q. *J. Phys. Chem. Solids* **1998**, *59*, 105.
(3) Hazen, R. M.; Finger, L. W.; Mariathasan, J. W. E. *J. Phys. Chem. Solids* **1985**, *46*, 253.
(4) Trunov, V. K.; Efremov, V. A.; Velikodnii, Yu. A. *Crystallography and properties of double molybdates and tungstenates*; Nauka: Leningrad, 1986 (in Russian).
(5) Evdokimov, A. A.; Efremov, V. A.; Trunov, V. K. *Compounds of the rare earth elements*; Nauka: Moscow, 1991 (in Russian).
(6) Klevtsov, P. V.; Klevtsova, R. F. *J. Struct. Chem.* **1977**, *18*, 339 (English translation).
(7) Klevtsov, P. V.; Protasova, V. I.; Kharchenko, L. Yu.; Klevtsova, R. F. *Crystallogr. Rep.* **1973**, *18*, 833 (in Russian).

10.1021/cm0605668 CCC: $33.50
Published on Web 07/28/2006

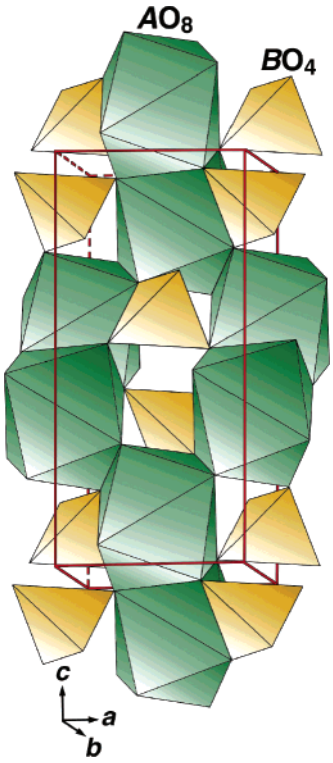

Figure 1. Polyhedral view of the scheelite-type structure.

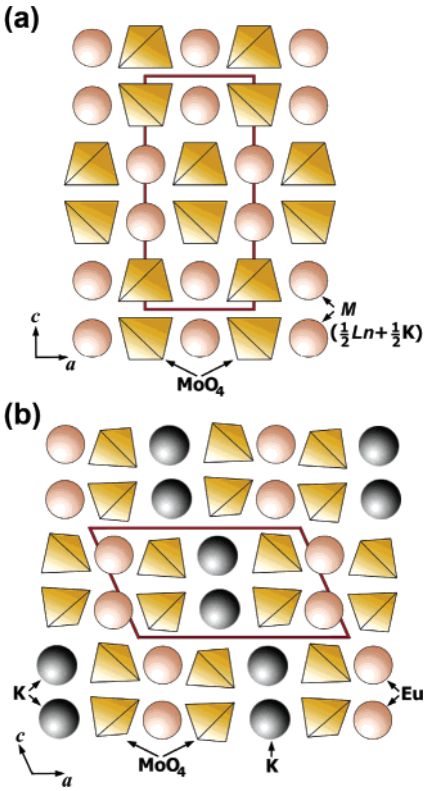

Figure 2. A layer of a scheelite-type structure with cations and MoO_4 tetrahedra: (a) statistical distribution of M^+ and R^{3+} at the A positions in the tetragonal structure of $MR(MoO_4)_2$ (M = Li, Na; R = Ln, Y, Bi); (b) ordered distribution of K^+ and Eu^{3+} in the α-$KEu(MoO_4)_2$ structure.

The $KR(MoO_4)_2$ double molybdates are mostly of interest because of their variety of crystal structures and the occurrence of polymorphism. For $KR(MoO_4)_2$ nine different modifications of the structure were found, depending on the size and nature of the rare earth element and the compound formation conditions.[4−6,8,9] In general, these compounds can be divided into two groups: (1) scheelite-type modifications including phases with an α-$KEu(MoO_4)_2$-type structure (space group $P\bar{1}$) and (2) non-scheelite modifications with the $KY(MoO_4)_2$-type structure (space group *Pbcn*). Despite the fact that $KR(MoO_4)_2$ double molybdates are known practically for all Ln elements, only the α-$KEu(MoO_4)_2$[10] and $KY(MoO_4)_2$[11] crystal structures have been studied in detail.

The formation of $KR(MoO_4)_2$ phases with the $KY(MoO_4)_2$-type structure is observed only for R = Dy−Lu. According to refs 4−6 and 8, $KR(MoO_4)_2$ (R = Dy−Tm) do not present phase transformations above room temperature up to the melting point under atmospheric pressure. However, for R = Dy, a modification with the α-$KEu(MoO_4)_2$-type distortion of the scheelite-type structure was found recently, whereas all attempts to obtain a similar $KR(MoO_4)_2$ modification for R = Y, Ho, and Er were unsuccessful.[12] $KR(MoO_4)_2$ phases with the α-$KEu(MoO_4)_2$ distorted scheelite-type structure are found only for R from Eu to Dy. In contrast to the tetragonal $MR(MoO_4)_2$ (M = Li, Na; R = Ln, Y, Bi) compounds with a statistical distribution of M^+ and R^{3+} in the structure, the K^+ and Eu^{3+} cations in α-$KEu(MoO_4)_2$ are ordered (Figure 2).

The data for the polymorphous modifications of $KR(MoO_4)_2$ (R = La−Sm) are limited and only refer to the syntheses and the determination of the supercell parameters. In the majority of investigations, the authors classified the $KR(MoO_4)_2$ (R = La−Sm) compounds as tetragonal scheelite-type phases[13] or suggested a monoclinic distortion. The α- and β-modifications of $KLa(MoO_4)_2$ were obtained by hydrothermal synthesis.[14,15] According to Potapova et al.,[15] the higher stability limit of the α-modification lies within 560−565 °C. X-ray powder diffraction patterns for α-$KLa(MoO_4)_2$ were indexed in a body-centered monoclinic subcell with unit cell parameters $a = 5.437(1)$ Å, $b = 12.205(2)$ Å, $c = 5.417(1)$ Å, and $\beta = 90.05(1)°$. Synthesis and indexing of the X-ray powder diffraction patterns of $KNd(MoO_4)_2$ (named as the γ-modification) were also reported,[16] although the lattice parameters and the monoclinic space group were not accurate or reliable (a small number of reflections analyzed and a low value of the figure-of-merit (F24 = 2)).

(8) Sokolovsky, B. M.; Evdokimov, A. A.; Trunov, V. K. *Zh. Neorg. Khim.* **1977**, *22*, 1499 (in Russian).
(9) Klevtsov, P. V.; Kozeeva, L. P. *Crystallogr. Rep.* **1976**, *21*, 316 (in Russian).
(10) Klevtsova, R. F.; Kozeeva, L. P.; Klevtsov, P. V. *Crystallogr. Rep.* **1974**, *19*, 83 (in Russian).
(11) Klevtsova, R. F.; Borisov, S. V. *Dokl. Acad. Nauk SSSR* **1967**, *177*, 1333 (English translation).
(12) Basovich, O. M.; Khaikina, E. G.; Solodovnikov, S. F.; Tsyrenova, G. D. *J. Solid State Chem.* **2005**, *178*, 1580.
(13) Powder Diffraction File, Cards 32-0804, 33-1035, and 51-1846 JCPDS, International Centre for Diffraction Data, 1601 Park Lane, Swarthmore, PA 19081.
(14) Protasova, V. I.; Kharchenko, L. Yu. *Zh. Neorg. Khim.* **1981**, *26*, 2271 (in Russian).
(15) Potapova, O. G.; Protasova, V. I.; Kharchenko, L. Yu. *Russ. J. Inorg. Chem. (Transl. of Zh. Neorg. Khim.)* **1987**, *32*, 1703.
(16) Bushuev, N. N.; Trunov, V. K.; Gizhinskii, A. R. *Zh. Neorg. Khim.* **1973**, *18*, 2865 (in Russian); *Russ. J. Inorg. Chem. (Transl. of Zh. Neorg. Khim.)* **1973**, *18*, 1523.

The aim of the present paper is to determine the structure of the incommensurately modulated scheelite-type structure of KNd(MoO$_4$)$_2$, which is the next example of an incommensurately modulated structure in the scheelite-like family after Ag$_{1/8}$Pr$_{5/8}$MoO$_4$.[17]

2. Experimental Section

The KNd(MoO$_4$)$_2$ double molybdate was prepared from a 1:1:3 stoichiometric mixture of K$_2$MoO$_4$ (99.99%), Nd$_2$O$_3$ (99.99%), and MoO$_3$ (99.99%), by a routine ceramic technique at 723−873 K for 80 h in air followed by quenching from 873 K to room temperature.

X-ray powder diffraction patterns for the structure refinement were collected at room temperature on a SIEMENS D500 diffractometer equipped with a primary SiO$_2$ monochromator (Cu Kα_1 radiation, $\lambda = 1.5406$ Å, Bragg−Brentano geometry) and a position-sensitive detector (BRAUN). The data were collected over the 2θ range 7−120° with steps of 0.02°. Rietveld analysis of the incommensurately modulated structure was performed using the JANA2000 program package.[18] All the illustrations were produced with the JANA2000 program package in combination with DIAMOND.[18]

Electron diffraction (ED) and high-resolution electron microscopy (HREM) investigations were made on crushed samples deposited on holey carbon grids. Energy-dispersive X-ray (EDX) analysis and ED patterns were obtained using a Philips CM20 microscope with a LINK-2000 attachment. For the EDX analysis, results were based on the K$_K$, Nd$_L$, and Mo$_L$ lines of the spectra. HREM observations were performed using a JEOL 4000 EX microscope operating at 400 kV. The Scherzer resolution of the microscope is 1.7 Å. Simulations of the HREM images were performed using the MacTempas software.

3. Results and Discussion

3.1. Elemental Composition. The elemental composition of KNd(MoO$_4$)$_2$ was confirmed by EDX analysis performed inside the transmission electron microscope and linked with the ED analysis for each crystallite. EDX was performed at 4 points for 10 different crystallites. The cation ratio was found to be K:Nd:Mo = 0.96(2):0.96(4):2.00(4) (24.7(4) atom % K, 24.2(8) atom % Nd, 51.0(8) atom % Mo). This is close to the bulk KNd(MoO$_4$)$_2$ composition and reveals a homogeneous element distribution in the sample.

3.2. Electron Diffraction Study. [1$\bar{1}$0]*, [111]*, [100]*, and [001]* ED patterns of KNd(MoO$_4$)$_2$ are shown in Figure 3. All reflections in the [1$\bar{1}$0]*, [111]*, and [100]* ED patterns are main reflections referring to tetragonal scheelite, space group $I4_1/a$, with unit cell parameters $a_t \approx 5.46$ Å and $c_t \approx 11.86$ Å. The reflections observed in the [001]* ED pattern are satellite reflections due to an incommensurate modulation of the scheelite-type structure with a modulation vector $\mathbf{q}_t \approx 0.58\mathbf{a}_t^* - 0.15\mathbf{b}_t^*$ (t indicates tetragonal cell). The symmetry of the modulation requires a monoclinic symmetry. Two different settings are possible: (1) B-centered unit cell with parameters $a \approx a_t\sqrt{2} \approx 7.62$ Å, $b \approx a_t \approx 5.33$ Å, $c \approx c_t \approx 11.74$ Å, and $\gamma \approx 134°$ and a modulation vector $\mathbf{q}$ having the approximate components $0.45\mathbf{a}^* - 0.15\mathbf{b}^*$; (2) I-centered unit cell with parameters $a \approx a_t$, $b \approx a_t$, $c \approx c_t$, and $\gamma \approx 90°$ and a modulation vector $\mathbf{q}$ having approximate components $0.58\mathbf{a}^* - 0.15\mathbf{b}^*$. $B2/b(\alpha\beta0)00$ is the conventional standard setting for the superspace group.[19] Nevertheless, the indexing of the ED patterns in the I-centered unit cell is more preferable because (1) the I-centered setting is a standard scheelite setting and (2) the γ angle is close to 90°. According to one of the standard crystallography rules, if a crystal structure can be described in two or more different monoclinic settings (space group, unit cell parameters, etc.), the setting with the minimal deviation of the monoclinic angle from 90° should be selected.

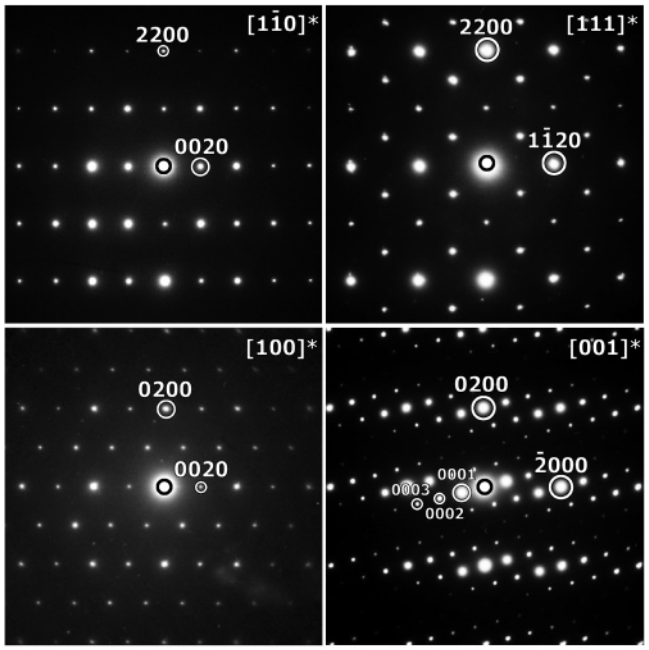

Figure 3. [1$\bar{1}$0]*, [111]*, [100]*, and [001]* ED patterns of the incommensurately modulated KNd(MoO$_4$)$_2$ phase.

The indexing of the ED patterns (Figure 3) was made with four *hklm* indices given by the diffraction vector $\mathbf{H} = h\mathbf{a}^* + k\mathbf{b}^* + l\mathbf{c}^* + m\mathbf{q}$, $\mathbf{q} = 0.58\mathbf{a}^* - 0.15\mathbf{b}^*$. The reflections with $m = 0$ and $m \neq 0$ correspond to the main and satellite reflections, respectively. All ED patterns can be completely indexed in the superspace group $I2/b(\alpha\beta0)00$ with the unique axis *c*. The [1$\bar{1}$0]*, [111]*, and [100]* diffraction patterns exhibit only main *hklm* reflections with $m = 0$.

The [1$\bar{1}$0]* and [111]* patterns exhibit *hk*00, *h*, $k \neq 2n$, reflections forbidden by the $I2/b$ symmetry. The intensity of these reflections, however, is systematically lower than the intensity of the *hk*00, *h*, $k = 2n$, reflections. On tilting the sample around the [*hk*00] direction, the reflections *hk*00, *h*, $k \neq 2n$, further weaken and finally vanish in the [001]* pattern. Consequently, these spots are attributed to double

(17) Morozov, V. A.; Mironov, A. V.; Lazoryak, B. I.; Khaikina, E. G.; Basovich, O. M.; Rossell, M. D.; Van Tendeloo, G. *J. Solid State Chem.* **2006**, *179*, 1172.

(18) (a) Petrícek, V.; Dusek M.; Palatinus, L. *JANA2000: the crystallographic computing system*; Institute of Physics: Praha, Czech Republic, 2000. (b) Dusek, M.; Petrícek, V.; Wunschel, M.; Dinnebier, R. E.; Van Smaalen, S. *J. Appl. Crystallogr.* **2001**, *34*, 398. (c) Petrícek, V.; van der Lee, A.; Evain, M. *Acta Crystallogr.* **1995**, *A51*, 529 (d) Brandenburg, K. *DIAMOND*, Version. 2.1c; Crystal Impact GbR: Bonn, Germany, 1999.

(19) Janssen, T.; Janner, A.; Looijenga-Vos, A.; De Wolff, P. M. Incommensurate and commensurate modulated structures. In *International Tables for Crystallography*; Wilson, A. J. C., Ed.; Kluwer Academic Publishers: Dordrecht, The Netherlands, 1995; Vol. C, pp 797−835.

Table 1. Crystal Data, Data Collection, and Refinement of $KNd(MoO_4)_2$

molecular formula	$KNd(MoO_4)_2$
fw	503.2
temp (K)	293(2)
cell setting	monoclinic
superspace group	$I2/b(\alpha\beta0)00$
lattice params	
a (Å)	5.5202(2)
b (Å)	5.33376(5)
c (Å)	11.8977(3)
γ (deg)	90.9591(7)
V (Å^3)	350.261(18)
q vector	$0.57789(4)\mathbf{a}^* - 0.14748(6)\mathbf{b}^*$
no. of formula units, Z	2
calcd density, D_c (g cm^{-3})	4.770(1)
color	light violet
Data Collection	
diffractometer	SIEMENS D500
radiation/wavelength (λ/Å)	Cu Kα_1/1.5406
radiation monochromator	primary SiO_2
abs coeff, μ (mm^{-1})	92.701
$F(000)$	454
2θ range (deg)	7−120
step scan (2θ)	0.02
I_{max}	50154
no. of points	5650
Refinement	
refinement	Rietveld
background function	Legendre polynomials, 12 terms
no. of reflns (all/obsd)	1826/1780
among them	
main	257/256
first-order satellites	525/520
second-order satellites	527/510
third-order satellites	518/495
no. of refined params/ refined atomic params	51/34
R and R_w (%) for Bragg reflections (R_{all}/R_{obsd})	3.59/3.41 and 2.65/2.64
among them	
main	2.17/2.14 and 1.87/1.87
first-order satellites	4.15/4.10 and 2.65/2.64
second-order satellites	5.03/4.62 and 3.08/3.07
third-order satellites	5.90/4.88 and 3.19/3.17
R_p, R_{wp}, R_{exp}	3.09, 4.04, 2.24
GOF (χ^2)	3.25
max/min residual density (e Å^{-3})	1.24/−1.61

diffraction and do not violate the $I2/b$ symmetry. No reflection conditions apply for the satellite reflections (with $m \neq 0$) besides the I-centering reflection conditions.

3.3. Refinement of the $KNd(MoO_4)_2$ Crystal Structure. The incommensurate scheelite-like structure of $KNd(MoO_4)_2$ has been refined from the powder diffraction intensities in the scheelite-like setting with the superspace group $I2/b(\alpha\beta0)00$ similar to the $Ag_{1/8}Pr_{5/8}MoO_4$ structure.[17] Following the refinement of the profile parameters (Table 1), the unit cell parameters and the **q** vector obtained by electron microscopy were refined as $a = 5.5202(2)$ Å, $b = 5.33376(5)$ Å, $c = 11.8977(3)$ Å, $\gamma = 90.9591(7)°$, and $\mathbf{q} \approx 0.578\mathbf{a}^* - 0.147\mathbf{b}^*$. The refinement of the unit cell characteristics, together with the profile parameters, allowed the indexing of 1826 intensities including main and satellite reflections up to the third order (Table 1). The positional, atomic displacements and modulation characteristics obtained for the Mo and O atoms in $Ag_{1/8}Pr_{5/8}MoO_4$[17] were used as the starting model. After refinement ($R_{all} \approx 22\%$), the residual electron density map was analyzed in the vicinity of the A

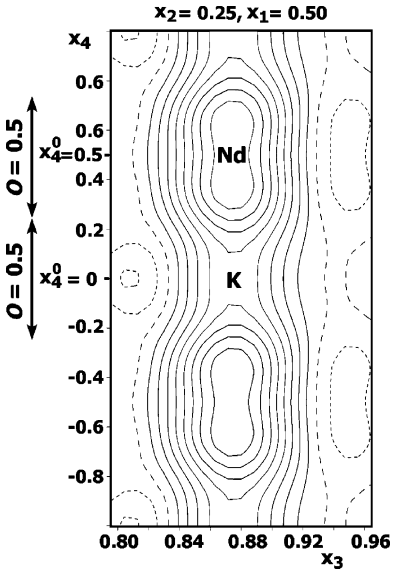

Figure 4. Determination of the modulation type of K and Nd located in the A position ($x_1 = 0.5$, $x_2 = 0.25$, $x_3 \approx 0.88$) using the x_3x_4 section of the residual electron density map. Both K and Nd atoms are successfully described by a Crenel function; i.e., they are located in the 0 ± 0.25 (K) and 0.5 ± 0.25 (Nd) ranges along the external x_4 axis. Each atomic domain is described by its center (x_4^0) and its extension (occupation, o). The residual electron density was calculated in the absence of K and Nd atoms. Full, dashed, and stippled lines correspond to positive, zero, and negative values of the electron density with 10 e/cm^3 steps, respectively.

cation on an x_3x_4 section (Figure 4) to determine the distribution function of the K and Nd atoms in superspace. According to this analysis, two Crenel functions (Figure 4) were chosen and successfully applied for the K and Nd atoms with parameters $x_4^0 = 0$ (K) and $x_4^0 = 0.5$ (Nd) and an occupation parameter $o = 0.5$ for both A atoms (Figure 4). The occupation parameters satisfying the results of the EDX analysis were fixed for further calculations. This structural model was successfully refined using isotropic atomic displacement parameters (ADPs). The large ratio of observations per refined parameter (1826/51 > 35.8) allowed the refinement of the anisotropic ADPs for all cations.

The reliability factors $R_{all} = 3.59\%$ and $R_p = 3.09\%$ show a good agreement between the calculated and the experimental profiles. Other numerical characteristics illustrating the quality of the structure refinement are presented in Table 1. The crystallographic parameters, atomic coordinates, modulation parameters and main relevant interatomic distances for $KNd(MoO_4)_2$ are listed in Tables 1−4. The experimental, calculated, and difference XRD patterns are shown in Figure 5.

Supplementary material has been sent to the Fachinformationzentrum Karlsruhe, Abt. PROKA, 76344 Eggenstein-Leopoldshaften, Germany, as supplementary material no. 416200 (97 pages) and can be obtained by contacting the FIZ (quoting the article details and the corresponding SUP number).

3.4. Specific Characteristics of the Incommensurate $KNd(MoO_4)_2$ Crystal Structure and Reasons for Its Modulation. The strong intensities of first-, second-, and third-order satellites, observed in the X-ray experiment, is a first significant characteristic of the incommensurately modulated scheelite-like $KNd(MoO_4)_2$ phase. As shown in

Table 2. Atomic Coordinates, Isotropic Displacement Parameters, and Fourier Amplitudes of the Displacive Modulation Function in KNd(MoO$_4$)$_2$

	harmonics[a]	*x*	*y*	*z*	U_{eq} (Å^2)
K[b]		0.5	0.25	0.8892(11)	0.017(3)
	s,1	−0.006(6)	−0.008(3)	0	
	c,1	0	0	−0.018(16)	
Nd[b]		0.5	0.25	0.8797(18)	0.0101(10)
	s,1	0.0018(16)	0.0268(10)	0	
	c,1	0	0	0.006(2)	
Mo		0.5	0.25	0.3774(2)	0.0157(11)
	s,1	0.0289(7)	−0.0048(7)	0	
	c,1	0	0	0.0109(4)	
O1		0.3599(10)	0.0203(12)	0.2928(5)	0.017(2)
	s,1	0.027(3)	0.008(3)	−0.0005(12)	
	c,1	−0.001(3)	0.020(3)	0.0070(11)	
O2		0.7744(13)	0.3936(10)	0.0429(5)	0.016(2)
	s,1	0.023(2)	−0.021(3)	0.0029(12)	
	c,1	0.030(3)	−0.004(3)	−0.0030(12)	

[a] Harmonics are listed by term (s for sinus, c for cosinus) and order *n*. [b] The Crenel function with occupation parameter $o = 0.5$ is used for both K ($x_4^0 = 0$) and Nd ($x_4^0 = 0.5$).

Table 3. Anisotropic Displacement Parameters in KNd(MoO$_4$)$_2$

	U^{11}	U^{22}	U^{33}	U^{12}	U^{13}	U^{23}
K	0.035(6)	0.002(6)	0.015(6)	−0.006(5)	0	0
Nd	0.0086(19)	0.0041(15)	0.017(2)	−0.0008(13)	0	0
Mo	0.0154(19)	0.0165(15)	0.015(2)	0.0044(14)	0	0

Table 4. Selected Cation−Oxygen Distances (Å) and Angles (deg) in the [MoO$_4$] Tetrahedra in KNd(MoO$_4$)$_2$

distance/ angle[a]	av	min	max
K−O1(i)	2.72(2)	2.59(3)	2.80(3)
K−O1(ii)	2.69(2)	2.63(2)	2.81(2)
K−O1(iii)	2.72(2)	2.59(3)	2.80(3)
K−O1(iv)	2.69(2)	2.63(2)	2.81(2)
K−O2(v)	2.65(2)	2.46(3)	2.752(18)
K−O2(vi)	2.74(2)	2.48(3)	2.846(18)
K−O2(vii)	2.65(2)	2.47(3)	2.752(18)
K−O2(viii)	2.74(2)	2.49(3)	2.846(18)
Nd−O1(i)	2.55(2)	2.49(2)	2.682(20)
Nd−O1(ii)	2.53(3)	2.47(3)	2.64(2)
Nd−O1(iii)	2.56(2)	2.49(2)	2.688(19)
Nd−O1(iv)	2.53(3)	2.47(3)	2.63(2)
Nd−O2(v)	2.55(3)	2.52(2)	2.63(2)
Nd−O2(vi)	2.53(2)	2.48(2)	2.63(2)
Nd−O2(vii)	2.56(3)	2.52(2)	2.63(2)
Nd−O2(viii)	2.53(2)	2.48(2)	2.64(2)
Mo−O1	1.757(17)	1.688(17)	1.827(17)
Mo−O1(x)	1.758(17)	1.688(17)	1.827(17)
Mo−O2(xiii)	1.755(16)	1.696(17)	1.809(17)
Mo−O2(xv)	1.753(16)	1.696(17)	1.809(17)
O1−Mo−O1(x)	110.0(8)	105.7(8)	114.5(8)
O1−Mo−O2(xiii)	108.3(8)	107.4(8)	109.5(8)
O1−Mo−O2(xv)	107.7(8)	105.6(8)	109.8(7)
O1(x)−Mo−O2(xiii)	107.8(8)	105.6(8)	109.8(7)
O1(x)−Mo−O2(xv)	108.3(8)	107.4(8)	109.5(8)
O2(xiii)−Mo−O2(xv)	114.4(7)	108.4(8)	120.7(8)

[a] (i) $1/2 + x$, $1/2 + y$, $1/2 + z$; (ii) $1 - x$, $-y$, $-1 - z$; (iii) $1/2 - x$, $1 - y$, $1/2 + z$; (iv) x, $1/2 + y$, $-1 - z$; (v) x, y, $1 + z$; (vi) $1 - x$, $1 - y$, $-1 - z$; (vii) $1 - x$, $1/2 - y$, $1 + z$; (viii) x, $-1/2 + y$, $-1 - z$.

Figure 5, some of them are much stronger than most of the main reflections. The series of strong low-angle reflections (see the inset in Figure 5) is an additional recognizable feature of the modulated scheelite-like structure. This series is also a characteristic of several powder diffraction patterns closely related to the incommensurately modulated KNd(MoO$_4$)$_2$ phase (Table 5). They can be found, but without

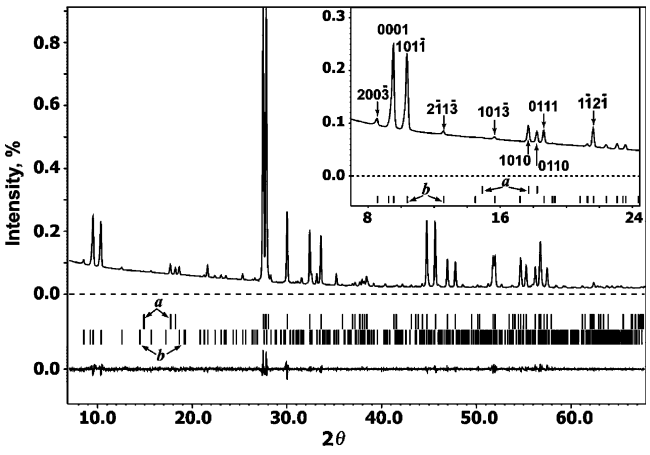

Figure 5. Experimental, calculated, and difference XRD patterns for KNd(MoO$_4$)$_2$. Tick marks denote the peak positions of possible Bragg reflections for (a) the main reflections and (b) the satellites. The inset shows a part of the profile with the indexation of some reflections. The pair of strong low-angle satellites is a characteristic feature of the scheelite-like incommensurate structures.

Table 5. Comparison between the Published Reflections[16] (Indexed in Space Group $P2_1/n$ with Unit Cell Parameters $a = 12.19$ Å, $b = 11.93$ Å, $c = 17.04$ Å, and $\gamma = 96.05°$) and the Indexation Corresponding to the Modulated Structure Model with the (3 + 1)*D* Monoclinic Superspace Group $I2/b(\alpha\beta0)00$

d (Å)	*I* (%)	*h k l*[16]	*d* (Å)	*I* (%)	*h k l m*
9.33	30	1 0 1	9.27	24	0 0 0 1
8.61	30	−1 1 0	8.52	22	1 0 1 −1
5.03	3	1 2 1	5.005	3	1 0 1 0
4.88	3	0 2 2	4.865	2	0 1 1 0
4.78	1	−2 1 2	4.757	2	0 1 1 1
4.10	3	0 2 3	4.108	4	−1 1 2 −1
3.250	100	1 2 4	3.2416	100	−1 1 2 0
3.21	100	−3 2 2	3.2036	100	1 1 2 0
2.981	40	0 4 0	2.9730	26	0 0 4 0
2.764	30	4 0 2	2.7595	19	2 0 0 0
2.667	30	−2 0 6	2.6662	17	0 2 0 0
2.557	10	2 2 5	2.5461	4	−2 1 3 −1, −1 1 2 1
			2.3571	2	−1 1 4 0
2.348	20	−3 4 2	2.3415	4	1 1 4 0
2.027	50	4 4 2	2.0226	26	2 0 4 0
1.989	50	−2 4 6	1.9850	26	0 2 4 0
1.937	10	2 0 8	1.9338	11	−2 2 0 0
1.904	10	1 6 2	1.9022	8	2 2 0 0
1.769	20	1 6 4	1.7671	4	−1 3 2 −1
1.762	20	4 3 6	1.7631	11	−1 1 6 0
1.680	10	5 2 6	1.6772	12	−3 1 2 0
1.664	10	−7 2 2	1.6610	10	3 1 2 0
1.637	10	−2 7 1	1.6345	10	−1 3 2 0
1.624	20	−1 7 3	1.62055	21	−2 2 4 0, 1 3 2 0
1.605	10	2 5 7	1.6018	9	2 2 4 0

indexing, in the JCPDS database for MLn(BO$_4$)$_2$ (M = alkali metal (Li, Na, K), Ln = lanthanide, B = W, Mo). The list of interplanar distances and corresponding intensities belonging to KEu(MoO$_4$)$_2$ (JCPDS PDF2 No. 31-1006) is shown in Table 6 as an example. The structural data obtained for KNd(MoO$_4$)$_2$ can directly be applied to these compounds. All reflections listed in Table 6 have been successfully indexed in the same monoclinic superspace group, $I2/b(\alpha\beta0)$-00, with unit cell parameters $a = 5.5241(17)$ Å, $b = 5.2864$-(15) Å, $c = 11.713(3)$ Å, and $\gamma = 91.247(17)°$ and $\mathbf{q} = 0.5641(2)\mathbf{a}^* - 0.1335(4)\mathbf{b}^*$. The JANA2000 program package was used for the unit cell refinement. Intensities of the reflections were estimated using the atomic characteristics for KNd(MoO$_4$)$_2$ with Nd replaced by Eu.

Table 6. Indexing of Reflections for $KEu(MoO_4)_2$ (JCPDS PDF2 No. 31-1006) in the $I2/b(\alpha\beta 0)00$ $(3+1)D$ Monoclinic Superspace Group with Unit Cell Parameters $a = 5.5241(17)$ Å, $b = 5.2864(15)$ Å, $c = 11.713(3)$ Å, and $\gamma = 91.247(17)°$ and $\mathbf{q} = 0.5641(2)\mathbf{a}^* - 0.1335(4)\mathbf{b}^*$

d_{exptl} (Å)	d_{calcd} (Å)	I_{exptl} (%)	I_{calcd} (%)	*h k l m*
9.6	9.55	30	28	0 0 0 1
8.4	8.38	30	24	1 0 1 −1
5.01	5.00, 4.99	10	3	1 0 1 0, 0 0 2 1
4.83	4.82	5	1	0 1 1 0
4.70	4.70	5	4	0 1 1 1
4.03	4.03, 3.99	10	7	1 −1 2 −1, 0 1 1 −1
3.506	3.49	5	3	1 1 2 −1
3.225	3.223	100	100	1 −1 2 0
3.176	3.174	100	100	1 1 2 0
2.930	2.928	50	27	0 0 4 0
2.807	2.800	5	3	0 0 4 1
2.765	2.761	50	22	2 0 0 0
2.693	2.689	20	5	1 1 2 1
2.641	2.643	50	20	0 2 0 0

An alternative description for the scheelite-like structures (Figure 6) is used here to analyze the specific features of the structure modulation observed in $KNd(MoO_4)_2$. [Using the JANA program package in combination with DIAMOND,[18] the following procedure has been applied for the incommensurate structure visualization: (i) starting with $t_0 = 0$, a portion of a $4 \times 4 \times 1$ unit cell has been selected for drawing; (ii) the positional parameters of all atoms appearing in the selected part have been calculated; (iii) this part of the structure is presented as a unit cell with *P*1 symmetry in CIF format and used for the structure visualization. This portion of the structure is not periodic and is not supposed to be translated in the aperiodic directions along *a* and *b*.] As shown in Figure 6a, the scheelite-like unit cell exhibits a distorted cubic face-centered (fcc) double cell with lattice parameter $a \approx 5.5 \pm 0.2$ Å for one fcc cell. In any scheelite-like structure, the A cations and BO_4 (MoO_4) groups are located at the junctions of the double fcc cell. Both ordered and disordered distribution of cations in fully or partially occupied A positions have been observed in the scheelite-like structures, while the B positions, i.e., the centers of the BO_4 groups, are topologically identical and fully occupied in all cases. As can be deduced from Figure 6b, an ordered distribution of K and Nd in the A position is periodic along the *c* axis but aperiodic (modulated) in the *ab* plane of $KNd(MoO_4)_2$. The ordering of K and Nd, observed as an occupation modulation of the A position, can be considered as the primary parameter of the structure modulation. Different crystal chemical properties of K and Nd (such as electron structure, ionic charge and radius, and ability for covalent bonding) require a different environment of the first coordination sphere populated by O atoms only. From the distance plot illustrated in Figure 7, we observe that the spread of the A−O distances along the internal coordinate *t* is larger for K−O values than for Nd−O values. In the same figure, we also observe that the MoO_4 tetrahedra tend to have stable Mo−O distances, indicating that they form rather rigid entities (Table 4). Figure 6c indicates that the MoO_4 groups have a tendency to get closer to the Nd atoms than to the K atoms. The diagrams represented in Figure 8 indicate also that the A cations only slightly deviate from their average positions whereas the Mo positions exhibit larger deviations.

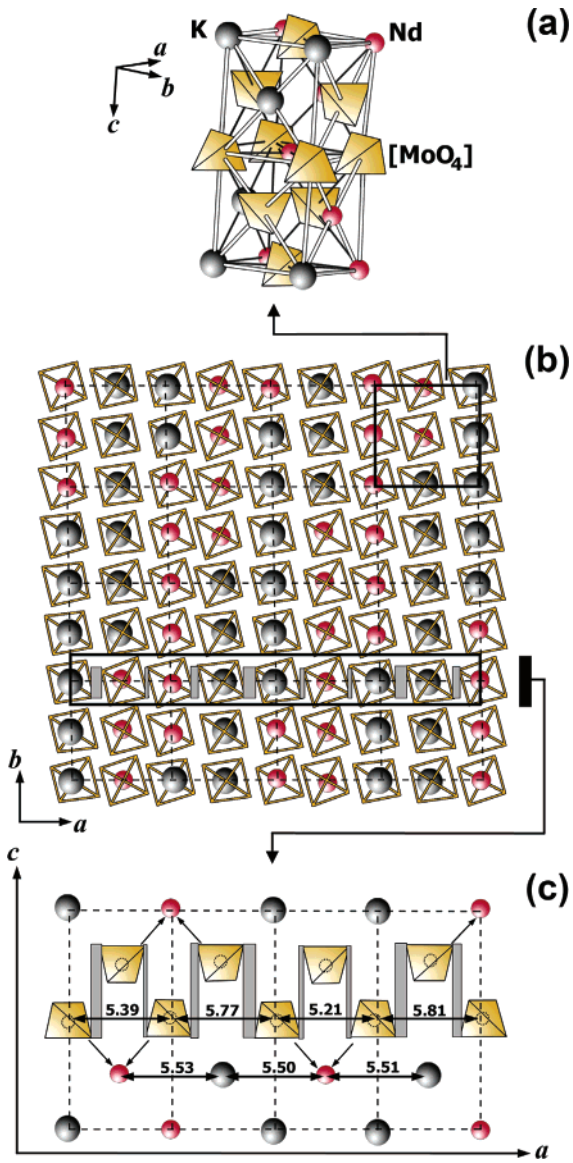

Figure 6. Specific features of the incommensurately modulated $KNd(MoO_4)_2$ structure: (a) an example of K (gray balls) and Nd (red balls) ordering in the A position of one scheelite-like unit cell shown as a distorted double fcc cell; (b) a portion of the aperiodic structure in the *ab* projection (dashed lines indicate the average unit cell); (c) a fragment of the structure illustrating the displacement (inclined arrows) of the MoO_4 tetrahedra toward the Nd atoms. The interatomic distances (the numbers above the double-arrow lines) A−A vary only slightly around the average value of 5.52 Å, while the Mo−Mo distances are significantly different (5.21−5.81 Å) owing to the MoO_4 displacements. The largest and the shortest tetrahedron displacements are represented by gray rectangular areas in (b) and (c). The width of the rectangles corresponds to their displacement along the *a* axis.

From this analysis we can conclude that the positional modulation of the MoO_4 rigid unit follows the occupation modulation of the A position; i.e., it is induced by the ordering of K and Nd in the A position.

The structure of $KNd(MoO_4)_2$ can be also interpreted in terms of columns of A cations and MoO_4 groups extending along the [001] direction as illustrated in Figure 6. Every column is formed of either $\{KMoO_4\}$ or $\{NdMoO_4\}$ units so that the distribution of K and Nd in the structure can be easily observed in the *ab* projection (Figure 6b) as a compositional wave extending in the direction of the vector $\mathbf{q} = \alpha\mathbf{a}^* + \beta\mathbf{b}^*$. Since α and β are irrational referring to

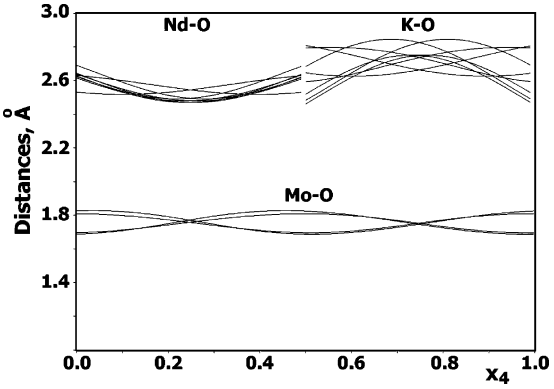

Figure 7. *t* dependence of the K−O, Nd−O, and Mo−O distances in KNd(MoO$_4$)$_2$.

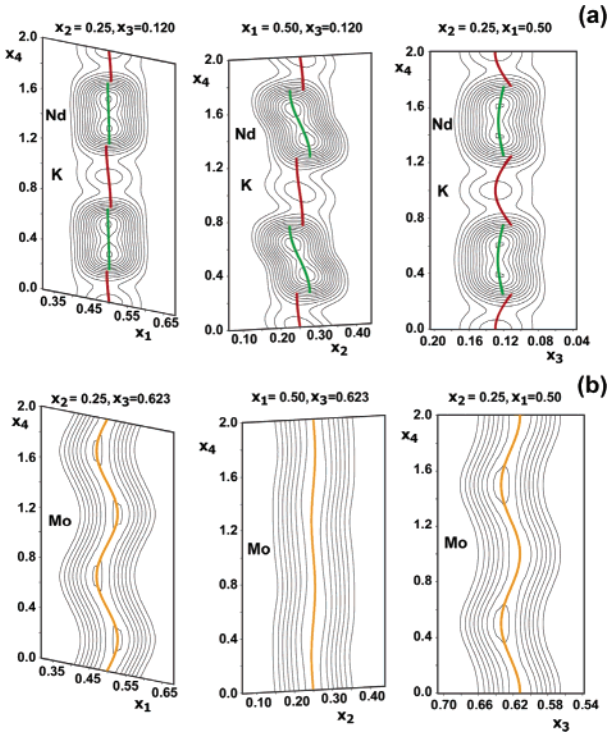

Figure 8. Positional modulations of K, Nd, and Mo in KNd(MoO$_4$)$_2$ as a function of the internal x_4 axis. The step between lines is 10 e/cm^3. The central colored lines correspond to the calculated atomic positions.

the *a* and *b* lattice parameters, the direction of the compositional wave is incommensurate with respect to them. The incommensurability of the compositional wave direction is thus at the origin of the incommensurability of the structure modulations.

A comparison of parts b and c of Figure 6 shows that the variation of the intercolumn distance is owed rather to the MoO_4 displacements than to the positions of K and Nd, which are practically unchanged. Knowing the affinity of MoO_4 toward the Nd atoms, the maximal and minimal distances will appear between two {$KMoO_4$} and two {$NdMoO_4$} columns, respectively. Therefore, the compositional wave can also be observed in the *ab* projection as a wave of inter-{$AMoO_4$}-column distances. This intercolumn distance variation is in perfect agreement with the high-resolution electron microscopy observations (Figure 9), discussed in the next paragraph.

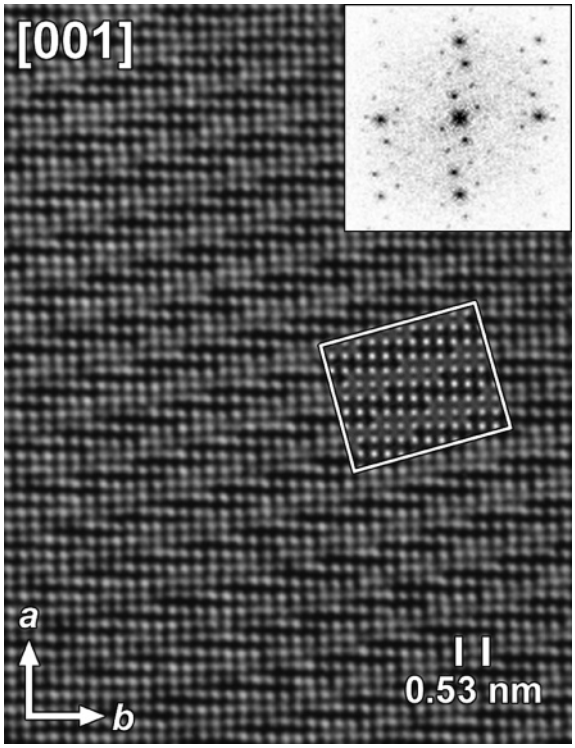

Figure 9. [001] HREM image and corresponding FT pattern of the incommensurate modulated KNd(MoO$_4$)$_2$ phase. The inset represents a calculated image based on the model of Figure 6b, for a focus value $\Delta f = -60$ nm and a thickness $t = 2$ nm.

3.5. High-Resolution Electron Microscopy Observation. HREM observations were performed at room temperature along the [001] direction. An image and the corresponding Fourier transform (FT) are shown in Figure 9. The FT pattern exhibits a spot distribution similar to that of the ED pattern in Figure 3, indicating that the modulation features have been imaged. The [001] HREM image consists of rows of bright dots corresponding to columns of {$KMoO_4$} and {$NdMoO_4$}. As discussed in the previous paragraph (Figure 6c), the maximum distance between two neighboring rows is observed for neighboring columns with K atoms. The distance between {$KMoO_4$} and {$NdMoO_4$} columns separated by a {$KMoO_4$} column is 5.71−5.81 Å, whereas the distance between the same columns separated by a {$NdMoO_4$} column is 5.21−5.39 Å. The difference between maximum and minimum column distances is ∼0.3−0.6 Å. This value is in agreement with the amplitude of the rows (∼0.2 Å) observed in the [001] HREM image. The wavelike character due to the variable intercolumn distance is clearly recognizable in Figure 9. In Figure 10b a portion of the *ab* structure projection (a portion of a 20 × 20 × 1 unit cell has been selected for structure visualization using the procedure described above) is shown using a comparable scale to illustrate the good correspondence between the projected structure and the HREM image (Figure 10a).

The distribution of the bright spots is not periodic along the *b* axis and may be described as a wave with a nonperiodic distribution of two distances between similar spots. One of them is equal to 7*b* (7 × 5.3 Å ≈ 37.1 Å), and the other is equal to 6.5*b* (6.5 × 5.3 Å ≈ 34.45 Å). Both kinds of distances are indicated in Figure 10. The aperiodic sequence

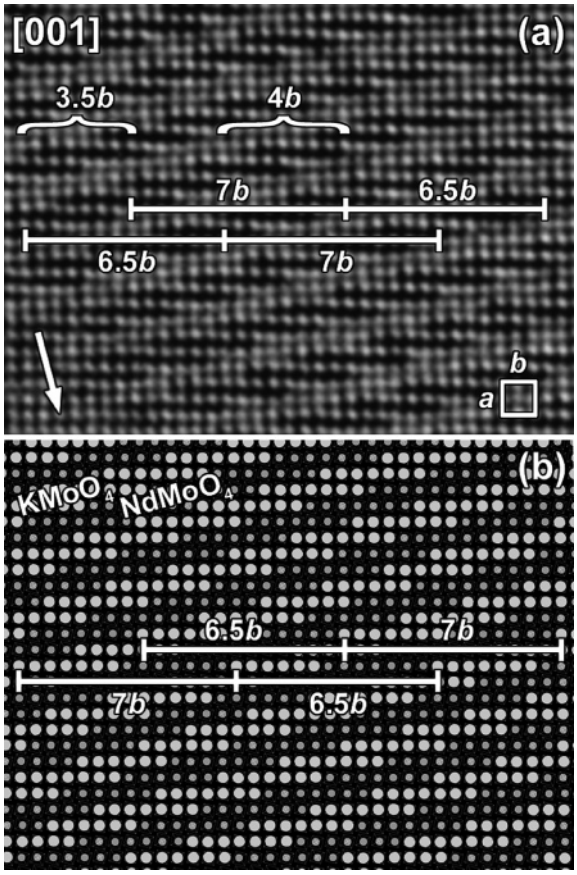

Figure 10. Comparison between (a) the experimental HREM image of $KNd(MoO_4)_2$ and (b) a schematic representation of the incommensurately modulated structure obtained from the crystal structure refinement showing the ordering of K^+ and Nd^{3+} cations. 7*b* and 6.5*b* indicate the distances between similar dots in a row along the *b* axis. The wavy rows are the results of shifts of every second layer by 4*b* or 3.5*b*. The arrow in (a) indicates the direction of the compositional wave.

of a "shorter" (6.5*b*) and a "longer" (7*b*) repeat period of the wave leads to the component $\beta\mathbf{b}^* = 0.147\mathbf{b}^*$ of the modulation vector $\mathbf{q} = \alpha\mathbf{a}^* - \beta\mathbf{b}^*$. Indeed, the value of the component $\beta\mathbf{b}^* = 0.147\mathbf{b}^*$ lies between $1/(7\mathbf{b}) = 0.142857\mathbf{b}^*$ and $1/(6.5\mathbf{b}) = 0.153846\mathbf{b}^*$.

Every second wavy row distant by *a* is shifted along the *b* axis by 4*b* or possibly 3.5*b* as observed in Figure 10. The nonperiodic alternation of the two displacements leads to the second component, $\alpha\mathbf{a}^* = 0.577\mathbf{a}^*$, of the modulation vector $\mathbf{q} = \alpha\mathbf{a}^* - \beta\mathbf{b}^*$. As can be deduced from Figure 10, the value of the component $\alpha\mathbf{a}^*$ lies between $(3.5b/7b)/\mathbf{a} = 0.5\mathbf{a}^*$ and $(4b/6.5b)/\mathbf{a} = 0.615384\mathbf{a}^*$ or more precisely between $3.5\beta/\mathbf{a} = 0.5145\mathbf{a}^*$ and $4\beta/\mathbf{a} = 0.588\mathbf{a}^*$. The more general relation $3.5\beta/\mathbf{a} < \alpha\mathbf{a}^* < 4\beta/\mathbf{a}$ or $3.5\beta < \alpha < 4\beta$ is therefore characteristic of $KNd(MoO_4)_2$. The value of $(1/\beta)b$ is the average length of the $\{AMoO_4\}$ wave in a row extending along *b*; α is the average shift of the wavy rows distant by *a*. α and β together define the direction of the compositional wave in the crystal as defined in the above paragraph (Figure 10). Since the structure modulation depends on the direction of the compositional wave and considering that the compositional wave can be attributed to the conditions of the crystal preparation, it can be concluded that, depending on the preparation, a variation of β between 1/6.5 and 1/7 as well as the corresponding variation of α can thus be expected for modulated structures with the same $KNd(MoO_4)_2$ composition.

4. Conclusion

The complex potassium neodymium molybdenum oxide, $KNd(MoO_4)_2$, was synthesized by a solid-state method and studied by X-ray and electron microscopy. Transmission electron microscopy revealed that the structure is incommensurate with $(3 + 1)D$ superspace group symmetry $I2/b(\alpha\beta0)00$ (unique axis *c*) and a modulation vector $\mathbf{q} \approx 0.58\mathbf{a}^* - 0.15\mathbf{b}^*$. The structure has been solved and refined by the Rietveld method from X-ray powder diffraction data. In this scheelite-like incommensurately modulated structure, ordering of the K and Nd cations induces a modulation of the MoO_4 tetrahedron positions. The distribution of K and Nd in the structure forms a compositional wave extending along $\mathbf{q} = \alpha\mathbf{a}^* + \beta\mathbf{b}^*$. The independence of the wave direction with respect to the *a* and *b* lattice constants can be regarded as the origin of the incommensurate character of the structure. On the basis of the structural features, we are also able to limit the range of possible α/β ratios for $KNd(MoO_4)_2$ and compounds with similar compositions.

Acknowledgment. This work has been performed within the framework of IAP V-1 of the Belgian Government. The contribution of the Swiss National Science Foundation, Grant Nos. 20-105325/1 and 200021-109470/1, is gratefully acknowledged.

CM0605668